Magnon-induced nuclear relaxation in the quantum critical region of a Heisenberg linear chain

M. J. R. Hoch

Phys. Rev. B **96**, 024444 — Published 27 July 2017

DOI: 10.1103/PhysRevB.96.024444

Magnon-induced nuclear relaxation in the quantum critical region of a Heisenberg linear chain

M.J.R. Hoch[1]

[1] *National High Magnetic Field Laboratory, Florida State University, Tallahassee FL 32310*

The low temperature properties of spin 1/2 one-dimensional (1D) Heisenberg antiferromagnetic (HAF) chains which have relatively small exchange couplings between the spins can be tuned using laboratory-scale magnetic fields. Magnetization measurements, made as a function of temperature, provide phase diagrams for these systems and establish the quantum critical point (QCP). The evolution of the spin dynamics behavior with temperature and applied field in the quantum critical (QC) region, near the QCP, is of particular interest and has been experimentally investigated in a number of 1D HAFs using neutron scattering and nuclear magnetic resonance as the preferred techniques. In the QC phase both quantum and thermal spin fluctuations are present. As a result of extended spin correlations in the chains, magnon excitations are important at finite temperatures. An expression for the NMR spin-lattice relaxation rate $1/T_1$ of probe nuclei in the QC phase of 1D HAFs is obtained by considering Raman scattering processes which induce nuclear spin flips. The relaxation rate expression, which involves the temperature and the chemical potential, predicts scaling behavior of $1/T_1$ consistent with recent experimental findings for quasi-1D HAF systems. A simple relationship between $1/T_1$ and the deviation of the magnetization from saturation (M_S-M) is predicted for the QC region.

The intriguing physical properties of one-dimensional (1D) Heisenberg antiferromagnet (HAF) systems which display quantum critical (QC) behavior and a quantum critical point (QCP) have been extensively discussed in the literature [1-5]. The ground state of a1D HAF spin S =1/2 chain, in a field somewhat lower than the QCP value $\mu_0 H_C$, is identified as aTomanaga-Luttinger-liquid (TLL). The TLL phase is characterized by spinon quasiparticles and spin correlation functions which exhibit quasi-long-range power law decay [6-9]. In addition, a TLL state is found in the gap-closed phase of the spin S = 1 Haldane chain. The QC phase, which is present at finite temperatures in the vicinity of the QCP, is of particular interest. In the QC region magnon excitations are important in accounting for changes in the magnetic and thermal properties with temperature and applied field. QC scaling behavior of the magnetization and other thermodynamic quantities is expected as a consequence of the key role played by the temperature in determining the energy scale [7-9].

Experimental investigations of the magnetization near the QCP have been carried out on a number of 1D HAF prototype systems such as Cu(C4H4N2)(NO2)3 (CuPzN) [8, 9] and the results are found to be consistent with scaling predictions. In addition, the dynamical properties of systems of this type have been studied using, primarily, neutron scattering [10-13] and nuclear magnetic resonance (NMR) [7,14-23]. These techniques provide information on changes in the spin dynamics close to the QCP. Low temperature NMR relaxation rates $1/T_1$ have, in particular, been shown to exhibit scaling based on a relationship involving empirical exponents which are determined in the data fit process [7]. In this note an expression is obtained for the temperature and magnetic field dependence of $1/T_1$ for a probe nucleus in a 1D HAF near the QCP by considering Raman magnon scattering processes in the QC phase. For a fixed applied field a scaling relationship for $1/T_1$ follows from the analysis.

The Hamiltonian for a 1D spin1/2 HAF is given by

$$\mathcal{H}_{\mathcal{S}} = J\sum_i \boldsymbol{S}_i \cdot \boldsymbol{S}_{i+1} - g\mu_0\mu_B H\sum_i S_i^z \,, \tag{1}$$

where J is the nearest neighbor (NN) intrachain exchange interaction for spins labeled i and j, μ_B is the Bohr magneton, and g the electron g-factor. Figure 1 shows a generic phase diagram for a HAF system of the type described by Eq. (1). The diagram is plotted using dimensionless reduced field H/H_C , and reduced temperature k_BT/J, variables where $\mu_0 H_C$ is the critical field. The straight lines separating the various regions represent crossovers between the TLL and QC phases for $H < H_C$ and between gapped and QC phases for $H > H_C$. For $k_BT/J > 0.5$ the quantum fluctuations become less important and the system transitions to paramagnetic behavior with increasing temperature. A detailed treatment of cross-over behavior in antiferromagnetic (AF) systems is given in Ref.24. The phase diagram in Fig. 1 does not include possible 3D AF order that may occur at low temperature, in low applied fields, as a result of weak interchain interactions with $J_{\text{inter}} \ll J_{\text{intra}}$. The Nćel temperature is suppressed in large applied fields which approach the saturation field in the vicinity of the QCP. Interchain interactions are therefore not considered in the present work which focuses on the QC phase.

In the QC region of a 1D HAF it is straightforward to derive an expression for the number of magnons, N_m , in a chain of length L in terms of the temperature and the chemical potential $\mu = g\mu_0\mu_B\left(H_C - H\right)$. Introducing the wave vector k, the magnon number is given by $N_m = \int_0^\infty dk\rho(k) f(\varepsilon_k - \mu)$. The Fermi distribution function $f(\varepsilon_k - \mu)$ is used because of the equivalence of a dilute1D Bose gas of magnons to a Fermi gas [5, 8]. The quadratic dispersion relation $\varepsilon(k) = \hbar^2 k^2 / 2m$ applies, with $m = \hbar^2 / J$ the effective mass [8]. The 1D density of states is given by $\rho(k) = L/\pi$. In terms of the variable $x = \sqrt{\hbar^2 k^2 / 2m\, k_B T}$ the following expression for the magnon density N_m / L is obtained:

$$\frac{N_m}{L} = \frac{\sqrt{2}}{\pi}\sqrt{\frac{k_B T}{J}}\int_0^\infty \frac{dx}{e^{x^2 - \mu/k_B T} + 1}. \tag{2}$$

The magnon contribution to the magnetization M is linked to N_m and this connection leads to the following expression for the difference between M and the saturation magnetization M_S [5, 8, 9],

$$\left(M_S - M\right) = \frac{\sqrt{2}}{\pi}\sqrt{\frac{k_B T}{J}}\int_0^{\infty}\frac{dx}{e^{x^{2-}-\mu/k_B T}+1} \quad . \tag{3}$$

Equation (3) provides the basis for scaled plots of $\left(M_S - M\right)/\sqrt{T}$ vs. $\mu/k_B T$ in the QC region for a particular system as shown recently for $Cu(C_4H_4)(NO_3)_2$ [9].

The bounds of the QC phase, which are indicated by the crossover lines in Fig.1, are established in terms of the chemical potential μ as follows. For $H < H_C$ the magnon density given in Eq.(2) passes through an extremum at temperature $T_m = 0.76238\mu/k_B$ which determines the QC –TLL crossover [6,8]. For $H > H_C$ an excitation gap is established and the crossover temperature to the QC region, as shown in Fig. 1, is taken as $T_g = \mu/k_B$ corresponding to significant occupation of states above the gap for $T > T_g$.

A scaling relationship for the NMR spin-lattice relaxation rate, $1/T_1$, is readily obtained for the QC phase of a 1D HAF if it is assumed that magnon scattering processes provide the relaxation mechanism in this region. The result obtained applies close to the QCP where $\mu_0 H$ produces quasi-ferromagnetic spin order. The Hamiltonian for electron spins S is given in Eq. (1) and that for nuclear spins I in an applied field $B = \mu_0 H$ is $\mathcal{H}_I = -\gamma_I \hbar \sum_n \boldsymbol{B_n} \cdot \boldsymbol{I}_n$ with γ_I the nuclear gyromagnetic ratio. The field $\boldsymbol{B_n}$ is the vector sum of the applied field $\boldsymbol{B}$ and the average local hyperfine field at nucleus n. It is convenient to assume that the general form of the Hamiltonian $\boldsymbol{S} \cdot \boldsymbol{A} \cdot \boldsymbol{I}$, in which $\boldsymbol{A}$ is the hyperfine tensor describing the electron-nucleus spin interaction, can be replaced by the scalar form $A\boldsymbol{I} \cdot \boldsymbol{S}$ with the effective hyperfine field making an angle θ with respect to the applied field direction. In this description, it is thermally induced fluctuations in the hyperfine component $A_{\perp} = A\sin\theta$ that gives rise to transitions between the nuclear spin states [25-27]. For spins $S = 1/2$, the anisotropy can arise as a result of dipolar interactions between I and S spins as discussed below.

Time dependent perturbation theory gives the following expression for the transition rate W between electron-nuclear spin states i and f produced by an interaction $\mathcal{H}_{\text{int}}$:

$$W = \frac{2\pi}{\hbar}\sum_{f}\left|\left\langle f\left|\mathcal{H}_{\text{int}}\right|i\right\rangle\right|^{2}\delta(\varepsilon_{i} - \varepsilon_{f'})\,. \tag{4}$$

The δ function ensures energy conservation with neglect of the small energy ($\sim 1\mu\text{eV}$) associated with a nuclear spin flip induced by the magnon scattering process. An expression for the spin-lattice relaxation rate is obtained by adapting the approach used in discussing nuclear spin-lattice relaxation due to Raman magnon scattering processes in three dimensions [25-27]. This involves use of the Holstein-Primakoff transformation with retention of just the term in the interaction which corresponds to the creation of a spin wave with wave vector $\boldsymbol{k}'$ and the destruction of a spin wave with wave vector $\boldsymbol{k}$. This approach gives the interaction Hamiltonian as [27],

$$\mathcal{H}_{\text{int}} = \frac{A_{\perp}}{2N} I^{+} \sum\nolimits_{\boldsymbol{k}',\boldsymbol{k}} \exp[i\left(\boldsymbol{k} - \boldsymbol{k}'\right)\cdot \boldsymbol{r}_{i}]a_{k'}^{\dagger}a_{k}\,, \tag{5}$$

where N is the number of spins in a chain, I^{+} the nuclear spin raising operator, $\boldsymbol{r}_{i}$ the position of spin i and $a_{k'}^{\dagger}$ and a_{k}, the spin wave creation and annihilation operators respectively.

For a 3D FM material the number of magnons, n_k, in a given energy state is given by the Bose-Eistein (BE) distribution function. In marked contrast, 1D HAF chains in the QC phase have the magnon number given by the Fermi-Dirac (FD) distribution as pointed out above. A given energy state for a QC 1D HAF can be either empty or singly occupied. In a nuclear relaxation magnon scattering process the change in k is extremely small and, to a very good approximation, $k = k'$. It follows that the exponential factor in Eq. (4) reduces to unity with the final state taken as equivalent to the initial state. The FD distribution is used together with the density of states in the sum over states in Eq.(4).

Using Eqs. (4) and (5), with summations over k replaced by integrals, the following expression for W in a1D HAF close to the QCP is obtained:

$$W = \frac{2\pi}{\hbar}\left(\frac{A_\perp}{2L}\right)^2 \int_0^{k_{\max}} \int_0^{k_{\max}} dk dk^{'} \rho(k)\rho(k^{'}) f(\varepsilon_k - \mu)\delta(\varepsilon_k - \varepsilon_{k^{'}}) . \tag{6}$$

Much of the notation is the same as that used in obtaining Eq.(2) with $k_{\max}$ the band edge value of k. Making use of the relation $1/T_1 = 2W$ gives the relaxation rate as:

$$\frac{1}{T_1} = \frac{4A_\perp^2}{\pi\hbar J}\sqrt{\frac{k_B T}{J}} \int_0^{\infty} \frac{dx}{e^{x^2 - \mu/k_B T} + 1}, \tag{7}$$

with $x = \sqrt{\hbar^2 k^2 / 2m\, k_B T}$ as before. The upper limit in the integral has been extended to infinity by assuming $k_B T < J$. It is convenient to introduce the frequencies $\omega_E = J/\hbar$ and $\omega_I = A_\perp/\hbar$ in order to write Eq. (7) in the form:

$$\frac{1}{T_1} = \frac{4\omega_I^2}{\pi\omega_E}\sqrt{\frac{k_B T}{J}} F\left(\frac{\mu}{k_B T}\right). \tag{8}$$

Equation (8) allows estimates to be made of $1/T_1$ in 1D HAFs as described below. Values of the function, $F(\mu/k_BT) = \int_0^\infty dx/(e^{x^2-\mu/k_BT}+1)$, are obtained by numerical integration.

In order to make estimates of the parameter ω_I in a particular HAF system it is necessary to consider the electron-nucleus interaction component $A_\perp$. In AF insulators it is often found that NMR experiments involve nuclei in non-magnetic spectator ions and not the nuclei of the magnetic ions themslves. This is because the magnetic ion nuclei experience fluctuations in the large contact hyperfine field and therefore have very short transverse and longitudinal relaxation times which make them unobservable in spin echo experiments. For NMR measurements involving spectator nuclei the electron spins *S* and the nuclear spins *I* may be coupled by transferred hyperfine interactions, with the form as given above in terms of $A_\perp$. In cases where the probe nuclei are not in the exchange path it is likely that the dipolar interaction is of dominant importance. It is possible that a combination of both transferred hyperfine and dipolar mechanisms apply in a particular material. In the dipolar case nuclear spin flips induced by the terms in the dipolar Hamiltonian $\mathcal{H}_{dip}$ which involve the raising or lowering *I* spin operators I^+ and I^-. These terms have the form $-\frac{3}{2}g\mu_B\gamma_I\hbar\sin\theta\cos\theta\exp(-i\phi)S_zI^\pm/r^3$ where θ and ϕ specify the orientation of the vector of length *r* connecting the spins [28, 29]. A summation over *S* spins is in general required in order to obtain an estimate of the fluctuating hyperfine field in a particular system. Procedures of this kind have been used, for example, for CuPzN [15]. In the present general discussion of magnon-induced nuclear relaxation ω_I is treated as a parameter.

From Eq. (8), the predicted behavior of $1/T_1$ as a function of *T* and *B* in the QC phase of a 1D HAF can be examined. Figure 2 is a dimensionless plot of C/T_1 vs. H/H_C where $C = \pi\omega_E/4\omega_I^2$, and

$H/H_C = 1 - \mu/g\mu_0\mu_B\, H_C$, with $\mu_0(H - H_C)$ in the range 0.3 to -0.3T. The plot takes $J/k_B = 10$ K and $\omega_E = J/\hbar$ = 1.3 x10^{12} s^{-1}. The critical field $B_C = 2J/g\mu_B$ is ~15 T for a spin1/2 HAF. An estimate of the order of magnitude of ω_I is obtained by assuming that the dipolar interaction between *I* and *S* spins is of dominant importance in the nuclear relaxation process. Taking $\gamma_I/2\pi$ ~ 10 MHz T^{-1} leads to $\omega_I \sim 10^6 - 10^7$ s^{-1}. For convenience a value C = 1 is used in the plot. Thus, knowledge of J, together with an estimate of ω_I, provides the basis for quantitatively predicting NMR relaxation rate behavior with temperature in the QC phase near the QCP of a 1D HAF chain.

It is interesting to note that the predicted forms for the relaxation rate variation with temperature given in Fig. 2 are very similar to the experimental behavior obtained in the vicinity of the QCP for the quasi-1D systems $NiCl_2$-4SC$(NH_2)_2$ (DTN) and $(C_5H_{12}N)_2CuBr_4$ (BPCB) presented in Ref.7. DTN has spin 1 chains while BPCB is a spin -1/2 ladder. It is argued that both systems are effectively spin-1/2 XXZ chains with anisotropic coupling J_Z/J_{XY} = 0.5 [7]. The scaling procedure which is applied to the DTN proton relaxation rate data in Ref.7 involves a plot of $1/T_1\, T^{\alpha}$ vs. $(B - B_C)/T^{\beta}$ using empirical exponents α and β. Best fit procedures give α = 0.46 $\pm\, 0.12$ and $\beta = 1.00 \pm 0.24$. It follows from the form of Eq. (8) that the $1/T_1$ values in the QC phase of a 1D HAF should exhibit scaling behavior with T using $F\left(\mu/k_B T\right)$ as the scaling function. The experimental results are therefore consistent with the magnon scattering model in which the exponents are determined as α =1 /2 and β = 1.

Figure 3 shows the magnon-induced behavior of $1/T_1$ as a function of $\mu/k_B\, T$ given by Eq. (8), again for $C = \pi\omega_E/4\omega_I^2$ = 1 and J / k_B = 10 K. A particular value of μ is used corresponding to a field slightly below $\mu_0 H_C$. The values obtained for $1 / T_1$ are ~ 0.15 – 0.3 s^{-1} for the constant C that is used. A smaller value for C (larger ω_I^2) will increase the relaxation rate. The inset in Fig. 3 is a plot of values of the scaling function $F(\mu/k_B T)$ vs. $\mu/k_B T$.

It is interesting to compare the relaxation rates for the two quasi-1D systems discussed in Ref. 7. At 1 K for $B \sim B_C$, the protons in DTN have $1/T_1$~100 s^{-1} while for ^{14}N in BPCB $1/T_1$~1 s^{-1} . Assuming that dipolar interactions are of primary importance for spin-lattice relaxation in both systems, it follows that the square of the ratio of the proton and carbon-13 gamma values $({}^{1}\gamma / {}^{14}\gamma)^2 \approx$ 600 is sufficiently large to more than account for the ratio of the measured $1/T_1$ values. It is necessary to bear in mind in testing data collapse predictions, involving temperature scaled data plots for a particular system, that it is implicitly assumed that the frequency ω_I, which is proportional to the amplitude of the fluctuating hyperfine field at the nuclear sites, remains constant for the limited range of fields and temperatures considered in the QC region. This assumption may not hold sufficiently well in some cases.

A comparison of Eqs.(3) and (8) shows that a relationship exists between the magnetization deviation from saturation $(M_S - M)$ and the spin-lattice relaxation rate in the QC phase of a 1D HAF.The relationship has the simple form $1/T_1 = K(M_S - M)$ with K a T-independent material specific constant. This interesting prediction, which follows from the NMR relaxation rate being proportional to the magnon density, should be tested by making $1/T_1$ and M measurements on a selected 1D HAF material.

The present analysis has focused on the NMR relaxation rate behavior in the QC region near the QCP of a 1D HAf as shown in Fig. 2. As the temperature is raised beyond 0.5 J/k_B thermally induced paramagnetic spin fluctuations become increasingly important giving $1/T_1 \propto T\chi_0$ with χ_0 the static susceptibility [14]. In the TLL phase in which spinon excitations determine the relaxation rate it has been shown that $1/T_1 \propto T^{-0.5}$ [17,20, 21]. Scaling behavior of $1/T_1$ with T has been examined in detail for the TLL phase as described for example in Ref. 30. In favorable cases it should be possible to follow the changes in the NMR relaxation rate dependence on temperature as crossovers occur from paramagnetic to QC or TLL regions of the phase diagram. It is clear that in 1D systems, including spin ladders and $S = 1$ Haldane chains with closed gaps, NMR provides a powerful means for exploring the crossover behavior. The magnon scattering model should be useful in analyzing muon spin-relaxation results obtained in μSR experiments on QC systems [31].

In conclusion, it is shown that magnon scattering processes, accompanied by nuclear spin flips, provide an NMR spin-lattice relaxation mechanism which is of dominant importance in the QC phase of a 1D HAF. The expression obtained for the relaxation rate involves the temperature, which sets the energy scale, and the chemical potential which determines the proximity to the QCP. In order to make quantitative predictions of relaxation rates it is necessary, firstly, to determine the QCP field $\mu_0 H_C$, and hence the exchange interaction J, and, secondly, to make an estimate of the fluctuating hyperfine field experienced by the nuclei used to probe the electron spin dynamics. Predictions based on the relaxation rate expression are found to be in broad agreement with experimental findings for two quasi-1D systems.

The work at the National High Magnetic Field Laboratory was supported by the NSF, under Cooperative Agreement No. DMR-1157490, and the State of Florida.

* hoch@magnet.fsu.edu

[1] S. Sachdev, *Quantum Phase Transitions*, 2nd ed. (Cambridge University Press, Cambridge, 2011).

[2] T. Giamarchi, *Quantum Phase Transitions in One Dimension* (Oxford University Press, Oxford, UK, (2004).

[3] S. Sachdev, Nature Physics **4**, 173 (2008).

[4] S. Sachdev and B. Keimar, Phys. Today **64**, No.2, 29 (2011).

[5] S. Sachdev, T. Senthil, and H. Shankar, Phys. Rev. B50, 258 (1994).

[6] Y. Maeda, C. Hotta, and M. Oshikawa, Phys. Rev. Lett. **99**, 057205 (2007).

[7] S. Mukhopadhyay, M. Klanjšek, M.S. Grbić, R. Blinder, H. Mayaffre, C. Berthier, M. Horvatić, M.A. Continentino, A. Paduan-Filho, B. Chiari, and O.Piovesana, Phys. Rev. Lett. **109**, 177206 (2012).

[8] Y. Kono, T.Sakibara, C.P. Aoyama, C. Hotta, M.M. Turnbull, C.P. Landee, and Y. Takano, Phys. Rev. Lett. **114**, 037202 (2015).

[9] M. Jeong, and H.M. Rømmow, Phys. Rev. B **92**, 180409(R) (2015).

[10] P.R. Hammar, M.B. Stone, D.H. Reich, C. Broholm, P.J. Gibson, M.M. Turnbull, C.P. Landee, M. Oshikawa, Phys. Rev. B **59**, 1008)1999).

[11] M.B. Stone, D.H. Reich, C. Broholm, K. Lefmann, C. Rischel, C.P. Landee, and M.M. Turnbull, Phys. Rev. Lett. **91**, 037205 (2003).

[12] M. Halg, D. Hüvonen, N.P. Butch, F. Demmel, and A. Zheludev, Phys. Rev. B **92**, 104416 (2015).

[13] K. Yu. Povarov, D. Schmidiger, N. Reynolds, R.Bewley, and a. Zheludev, Phys. Rev.B **91**, 020406(R) (2015).

[14] T. Goto, T. Ishikawa, and Y. Shimaoka, Phys. Rev. B **73**, 214406 (2006).

[15] H. Kühne, H.-H. Klaus, S. Grossjohann, W. Brenig, F.J. Litterst, A.P. Reyes, P.L. Kuhns, M.M. Turnbull, and C.P. Landee, Phys. Rev. B **80**, 045110 (2009).

[16] H. Kühne, A.A. Zvyagin, M. Günther, A.P. Reyes, P.L. Kuhns, M.M.Turnbull, C.P. Landee, and H.-H. Klaus, Phys. Rev. B **83**, 100407(R) (2011).

[17] R. Chitra, and T. Giamarchi, Phys. Rev. B **55**, 5816 (1997).

[18] E. Orignac, R. Citro, and T. Giamarchi, Phys. Rev. B **75**, 1404030(R) (2007).

[19] M. Jeong, H.Mayaffre, C. Berthier, D. Schimidiger, A. Zheludev, and M. Horvatić, Phys. Rev. Lett. **111**, 106404 (2013).

[20] M. Dupont, S. Capponi, and N. Laflorencie, Phys. Rev. B **94**, 144409 (2016).

[21] E. Coira, P. Barmettler, T. Giamarchi, and C. Kollath, Phys. Rev. B **94**, 14408 (2016).

[22] W. Kinross, M. Fu, T.J. Munsie H.A. Dabkowska, G.M. Luke, S.Sachdev,and T. Imai, Phys. Rev. X **4**, 031008 (2014).

[23] B. Dóra, M. Gulácsi, F. Simon, and H. Kuzmay. Phys. Rev. Lett**.** **99**, 166402 (2007).

[24] O.A.Starykh, H. Katsura and L. Balents, Physical Review B **82**, 014421 (2010).

[25] J. Van Kranaendonk, and M. Bloom, Physica **22**, 545 (1956).

[26] A.H. Mitchell, J. Chem. Phys. **27**, 17 (1957).

[27] D. Beeman, and P. Pincus, Phys. Rev. **166**, 359 (1968).

[28] A. Abragam, *The Princilples of Nuclear Magnetism*, (Clarendon Press, Oxford, 1961).

[29] C.P. Slichter, *Principles of Magnetic resonance*, 3rd ed. (Springer, Heidelberg, 1996).

[30] M. Takigawa, O.A. Starykh, A.W. Sandvik, and R.P. Singh, Phys. Rev. B **56**, 13681 (1997).

[31] J.s. M□ller, T. Lancaster, S.J. Blundell, F.L. Pratt, P.J. Baker, F. Xiao, R.C. Williams, W. Hayes, M.M. Turnbull, C.P. and Landee, Phys. Rev. B **95**, 0204020® (2017).

Figure captions

FIG. 1 (color online). Representative phase diagram for a 1D HAFin a dimensionless representation k_BT/J vs. $\mu/k_B\,T$ where J is the exchange coupling between NN spins and $\mu = g\mu_0\mu_B(H_C - H)$ is the chemical potential. . The QCP occurs at $\mu = 0$ and the straight lines which meet at this point represent crossover boundaries between TLL, QC and gapped phases as indicated. For $k_BT/J > 0.5$ the system transitions to its paramagnetic phase with rise temperature.

FIG. 2 (color online). Predicted behavior, based on Eq. (7), of the scaled NMR spin-lattice relaxation rate C/T_1 as a function of temperature in the QC phase for a 1D HAF. A Raman scattering mechanism is used in deriving Eq. (8). The parameter $C = 1/(4\omega_I^2/\pi\omega_E)$ where $\omega_I = A_\perp/\hbar$, with $A_\perp$ the amplitude of transverse component of the fluctuating hyperfine interaction, and $\omega_E = J/\hbar$. In the plot it is assumed, for convenience, that $C = 1$ and J/k_B =10 K. If NMR probe nuclei do not lie in superexchange paths the hyperfine coupling is likely to be dominated by the dipolar interaction between S and I spins.

FIG. 3 (color online).The predicted NMR spin-lattice relaxation rate $1/T_1$ as a function of $\mu/k_B\,T$ for two-magnon scattering processes in the QC phase of a 1D HAF obtained using Eq. (8). A particular value of μ, just below the QCP, is used, corresponding to $(H_C - H)/H_C = 0.01$, with $C = 1$, and J/k_B = 10 K. The inset shows a plot of the scaling function $F(\mu/k_B\,T)$ vs. $\mu/k_B\,T$ for the same μ value.

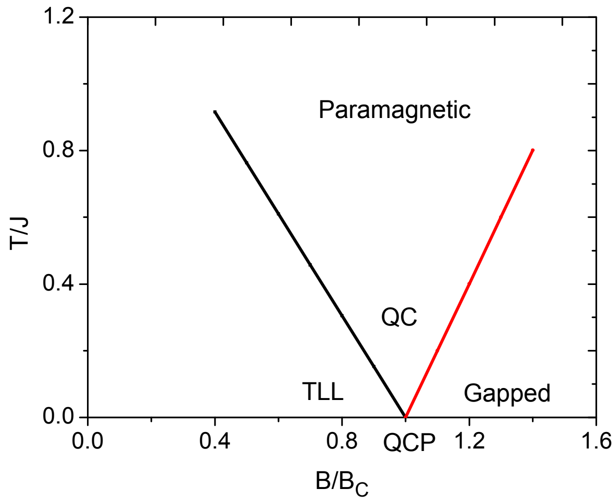
1.2
0.8
0.4
0.0
T/J
Paramagnetic
QC
TLL
Gapped
0.0
0.4
0.8
QCP
1.2
1.6
B/B_C

FIG. 1

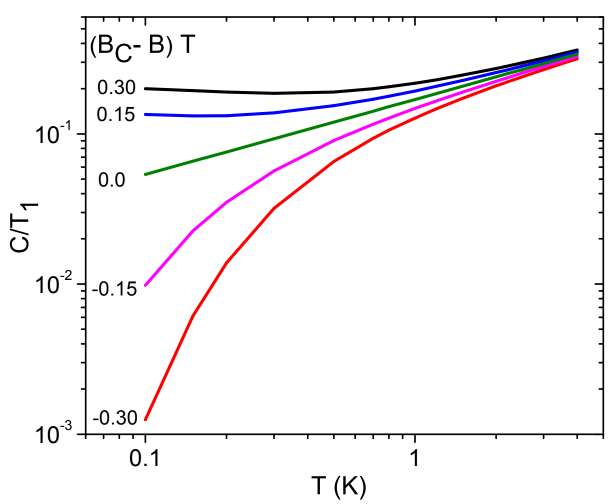
(B_C- B) T
0.30
0.15
0.0
-0.15
-0.30
10^-1
10^-2
10^-3
C/T_1
0.1
1
T (K)

FIG. 2

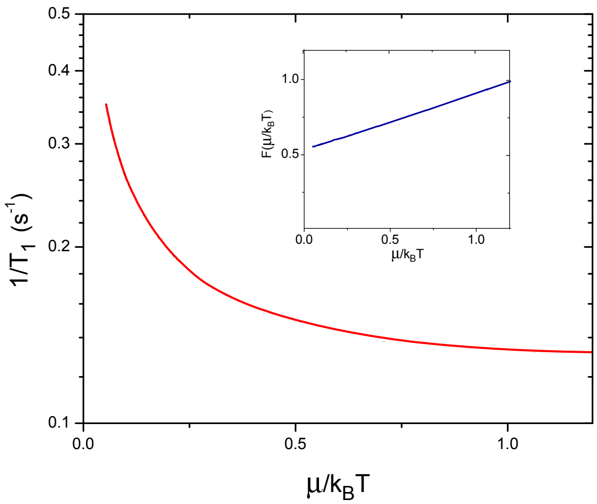

FIG. 3